Case Studies in Construction Materials 15 (2021) e00576

Contents lists available at ScienceDirect

Case Studies in Construction Materials

journal homepage: www.elsevier.com/locate/cscm

Development and characterization of clinoptilolite-, mordenite-, and analcime-based geopolymers: A comparative study

Didem Güngör, Sevgi Özen *

Recep Tayyip Erdoğan University, Geological Engineering Department, Rize, Turkey

ARTICLE INFO

Keywords:
Geopolymer
Clinoptilolite
Mordenite
Analcime
Compressive strength
Microstructure

ABSTRACT

This study examines the development of geopolymers from clinoptilolite, mordenite, and analcime and compares the properties of the resulting green-binding materials. Sodium silicate and sodium hydroxide solutions were used as activators. Compressive-strength, X-ray diffractometer (XRD), and scanning electron microscopy (SEM/EDX) analysis were employed to characterize the mechanical development, mineralogical composition, and microstructure of the geopolymers. The results show that clinoptilolite, mordenite, and analcime were found to offer much potential for the synthesis of geopolymers. Clinoptilolite-based geopolymer is the most reactive of the three and generates a higher rate of geopolymerization than mordenite- and analcime-based geopolymers. Reactive components other than zeolites are also found to be critical to the geopolymerization reaction. Feldspar provides additional Na for the reaction, reinforcing the gel structure and developing better compressive strength. The difference in the mechanical and microstructural properties of natural zeolite-based geopolymers is attributed to the varying nature and mineralogical content of the starting materials. Different gel characteristics provide valuable information on the role of the active phases involved in the reaction.

1. Introduction

Geopolymers with the potential of reducing the carbon footprint have attracted extensive attention of the researchers as a possible replacement of ordinary Portland cement (OPC) in construction product [1–3]. As a result of the assessment of the life cycle impact of geopolymers in comparison with OPC, it is stated that the CO_2 emissions from geopolymer concrete can be 97 % lower up to 14 % higher [4]. Compared to Portland cement, geopolymers also possess superior fire resistance, high early strength, high durability, low shrinkage, and low permeability [5]. Besides, geopolymers have excellent potential for application, such as civil engineering, metallurgy, nuclear waste management, heavy metal removal, inorganic membranes, aerospace fields, etc. [6–10].

Geopolymers can be considered as a member of the silicoaluminate family as synthetic zeolites. Although the chemical composition of geopolymers is similar to that of zeolitic materials, they are amorphous to semi-crystalline. Geopolymers can be synthesized by activating raw materials rich in Si and Al to a highly-alkaline liquid, such as sodium hydroxide (NaOH), potassium hydroxide (KOH), sodium silicate and potassium silicate. In a strong alkaline medium, the dissolution of aluminosilicate reactive material occurs, and polysialate, polysialate-siloxo, and polysialate-disiloxo—types of geopolymeric product—are formed [11]. These properties depend on many factors, such as the concentration of the activators, curing temperature, nature of the aluminosilicate materials [11]. In fact, the type of aluminosilicate source material plays an important role in the progress and development of the geopolymerization reaction,

* Corresponding author.
E-mail address: sevgi.ozen@erdogan.edu.tr (S. Özen).

https://doi.org/10.1016/j.cscm.2021.e00576
Received 4 March 2021; Received in revised form 22 April 2021; Accepted 13 May 2021
Available online 15 May 2021
2214-5095/© 2021 The Author(s). Published by Elsevier Ltd. This is an open access article under the CC BY-NC-ND license (http://creativecommons.org/licenses/by-nc-nd/4.0/).

controlling the chemical composition and microstructural development of the geopolymeric products. Furthermore, the main component of geopolymers, an aluminosilicate source, can be select from many starting materials including blast furnace slag [12–14], fly ash [11,15,16], metakaolin [17,18], volcanic ash [19,20] or natural zeolites [21–26], which in turn gives a flexibility in material selection that enable researcher to prefer, for example, locally available materials.

Natural zeolites are one of the most common and promising industrial minerals, with broad applications in agriculture, environmental and civil engineering. Besides, it was showed that they have a potential to produce geopolymer cement with reasonable strength. Villa et al. [22] determined the effect of the curing temperature and activator ratio on the compressive strength of clinoptilolite-based geopolymer, concluding that zeolitic materials can undergo geopolymerization and that geopolymeric materials cured at 40 °C showed the highest compressive strength. Bondar et al. [27] investigated the effect of the type, form, and dosage of the activators on the strength of a geopolymer manufactured using an Iranian natural pozzolan called Taftan andesite and Shahindej dacite, which is partly composed of clinoptilolite. Their results showed that the potassium hydroxide solution achieved optimal activation of the natural pozzolans between 5 M and 7.5 M, and 60 °C was the optimal curing temperature for the highest compressive strength. The effect of Jordanian natural zeolites, which belong to the phillipsite type, as a filler for the physical and mechanical properties and adsorption capacity of geopolymers has been studied by Yousef et al. [28]. They determined that natural zeolite-based geopolymers produce high compressive strength and a high adsorption capacity when in contact with methylene blue and copper (II) ions. In their study of mordenite-based geopolymers, Baykara et al. [24] concluded that the highest compressive strength of geopolymers was found under the following conditions: NaOH: 10 M, $Na_4Si_5O_{12}$/NaOH ratio: 0.5, $Ca(OH)_2$: 3% (w/w), and 60 °C. Nikolov et al. [25], synthesized calcined natural zeolite (clinoptilolite)-based geopolymer pastes using different alkaline activators, namely potassium hydroxide (KOH), potassium silicate (K_2SiO_3), sodium aluminate ($NaAlO_2$) and aluminium anodising waste solution. The test results demonstrated that maximum compressive strength was achieved for geopolymer pastes activated with KOH and K_2SiO_3. Tekin [23] prepared quarry waste volcanic tuff (containing clinoptilolite), travertine and marble-based geopolymers by activation with sodium silicate and sodium hydroxide. The resulting geopolymer pastes achieved sufficient compressive strength. It was stated that wet curing regimes cannot be used to produce geopolymers because of efflorescence problems.

As the literature review above shows, various studies on natural zeolite-based geopolymers have created a considerable amount of knowledge about the characteristics of resulting geopolymers. Yet, there is a need for examination of zeolitic tuffs on the consideration of the detail mineralogical composition. The co-existence of zeolite minerals (purity) and types of impurities (e.g. feldspar) is required to take into consideration to understand the underlying reactivity of geopolymers. Moreover, a literature search revealed no report on analcime-based geopolymers or results concerning their comparative studies. A study comparing different zeolite-based geopolymers created using the same mixing procedure would contribute important data to the existing literature. Therefore, geopolymers based on clinoptilolite-, mordenite-, and analcime-bearing tuff were examined for possible application as building materials. This study is important since clinoptilolite, mordenite and analcime, which are the most common zeolite species with high reserve capacity is an alternative raw material for industrial by-products such as fly ash and blast furnace slag, which led to availability problem for geopolymer production. Therefore, this study aims to examine the synthesis of geopolymers using clinoptilolite, mordenite, and

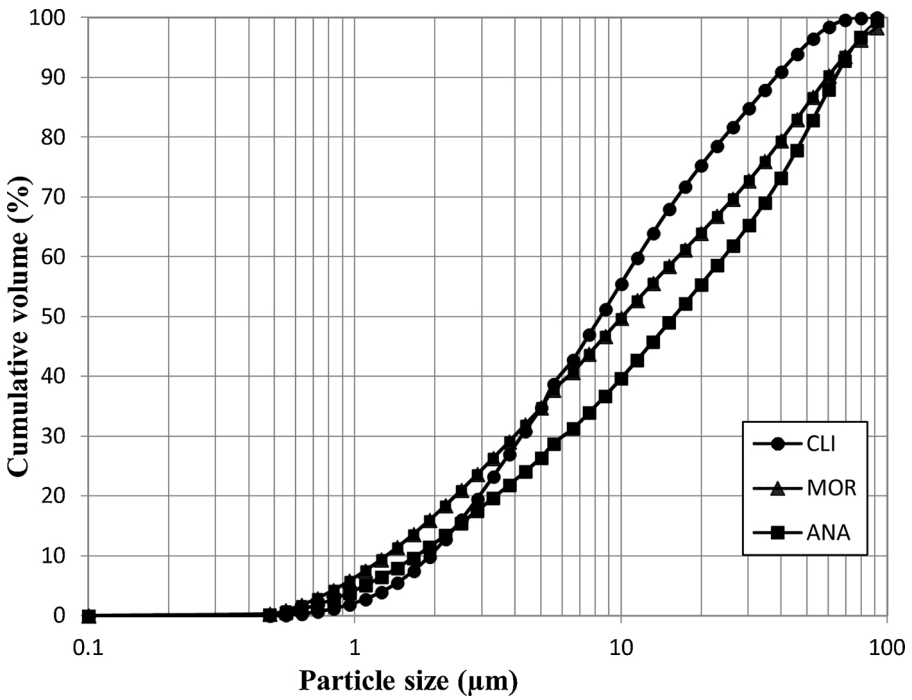

Fig. 1. Cumulative particle-size distributions of the zeolite-bearing tuffs.

Table 1
Chemical composition and physical properties of the examined tuffs.

	CLI	MOR	ANA
Chemical Compositions (%)			
SiO_2	67.87	70.82	60.81
Al_2O_3	10.46	11.19	19.47
Fe_2O_3	1.01	0.29	0.27
CaO	3.55	2.29	0.46
MgO	0.95	0.29	0.21
Na_2O	0.24	1.48	10.37
K_2O	1.93	2.13	0.28
MnO	0.05	0.03	0.02
L.O.I.	13.94	11.48	8.11
Total	100.00	100.00	100.00
Physical Properties			
Specific Gravity	2.11	2.12	2.27
Fineness (< 45 μm,%)	94.00	83.00	78.00
Fineness (Blaine, m^2/kg)	797	673	520
BET surface area (m^2/g)	40.13	12.13	9.51

analcime—common species of natural zeolites—as starting materials and compare the mechanical and microstructural properties of the three geopolymers by analyzing the resulting geopolymers with the aid of compressive strength, XRD and SEM/EDX analysis. It focuses particularly on the microstructure and composition of the final geopolymers, which play a vital role in understanding the behavior of the active phases and, therefore, of the compressive strength. The effect of reactive components other than zeolites in the source materials is also considered by SEM/EDX analysis.

2. Materials and methods

2.1. Raw materials

In this study, three zeolitic tuffs collected from the main zeolite deposits in western Turkey were used as a solid precursor. The clinoptilolite-rich tuff (CLI) was from Gordes, Manisa, the mordenite-bearing tuff (MOR) from Foca, Izmir, and the analcime-bearing tuff (ANA) from Kucukkuyu, Canakkale. CLI sample was collected from the lower Miocene Gokyar Tuff (Gordes Formation). MOR sample from the Yuntdag Group was found in the Middle Miocene Foca Tuff. ANA sample, on the other hand, was obtained from the Lower-Middle Miocene Arikli Tuff (Behram Volcanics) [29]. The samples were ground using a ball mill (MG171 Automatic Swing Mill). A water glass (Na_2SiO_3) solution, with a chemical composition of 27.7 % SiO_2, 9.8 % Na_2O, and 62.5 % H_2O by mass, and analytical-grade sodium hydroxide (NaOH) were used as the alkaline activators. The molar concentration of the NaOH solution was 12 M. Dissolved sodium hydroxide flakes with 98 purity were used to acquire the necessary concentration.

Particle size analyses shown in Fig. 1 with the following sequence: CLI < MOR < ANA were carried out with the laser diffraction method (Malvern Mastersizer 2000). The chemical composition of the zeolitic tuffs was examined using X-ray fluorescence (XRF; Rigaku ZSX Primus II) analysis, with the results given in Table 1. According to the results of the XRF analysis, the total SiO_2 and Al_2O_3 content of all three samples ranges from 78.33–80.28. CLI is characterized by a higher CaO value (3.55 %), and MOR by a higher K_2O (2.13 %) value, while ANA possesses higher Na_2O content (10.37 %). The physical properties of the raw materials are also shown in Table 1. The specific surface area was measured by N_2 adsorption, using the Brunauer–Emmett–Teller (BET) method (Quantachrome Corporation, Autosorb-6), after the activation of the zeolitic tuff samples under vacuum at 150 °C for 5 h and blaine fineness was measured in accordance with the ASTM C204 standard method [30]. As seen in Table 1, the order of the Blaine and BET values, from highest to lowest, is as follows: CLI, MOR, and ANA. The higher specific gravity of ANA is attributed to its large amounts of feldspar (40 %).

Quantitative phase analysis was performed using X-ray powder diffraction (XRPD) analysis in order to interpret the geopolymeric behavior of the not only zeolite minerals but also impurities. The samples with a grain size < 10 μm were ground for 15 min in a McCrone micronizing mill (agate cylinders and wet grinding). An α-Al_2O_3 (1 μm, Buehler Micropolish) was used as the internal standard (20 wt.%). Laboratory measurements were performed using a PANalytical X'Pert Pro device and X'Pert High Score Plus 3.0 software with CuKα radiation at 40 mA and 40 kV. The readings were recorded in vertical Bragg-Brentano geometry from 3 to 80° 2θ, with a step size of 0.0179° 2θ and 120 s counting time per step. The data sets were analyzed with the full profile Relative Intensity Ratio (RIR)/Rietveld method [31] implemented in the TOPAS 4.2 software (BRUKER AXS Company). The X'Pert High Score Plus 3.0 software was employed for the major and minor phase quantification procedure.

The qualitative-phase analysis of the zeolitic tuff and zeolite-based geopolymer samples was carried out with X-ray diffraction (XRD) analysis (after crushing and sieving the samples to obtain particles smaller than 63 μm) using a Philips PW 1730 diffractometer with Ni-filtered, CuKα1 radiation, operating at 40 kV, 30 mA.

Zeolitic tuffs were optically examined under a Nikon polarizing microscope to identify the mineralogy and relevant petrographic features. The morphology and microstructure of the samples were observed with a scanning electron microscope (SEM; QUANTA 400 F). Zeolite-based geopolymers had previously been coated with Au film. An energy dispersive X-ray spectroscopy (EDX) was used to

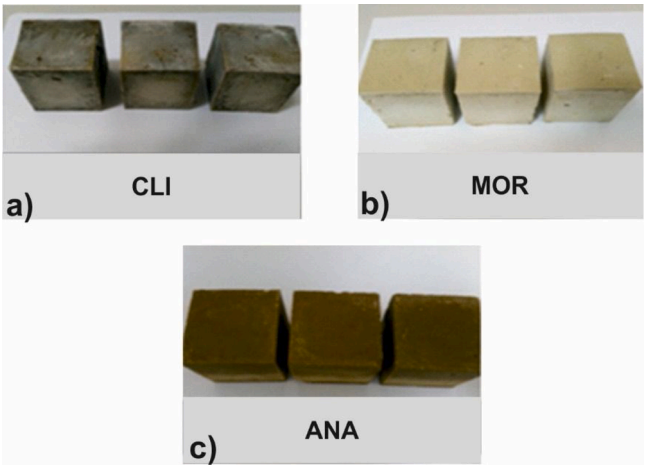

Fig. 2. Clinoptilolite-, mordenite-, and analcime-based geopolymers (CLI, MOR, ANA, respectively), which were cast in a 50 × 50 × 50 mm cube mold.

analyze the semi-quantitative elemental composition of the specimens' surfaces.

2.2. Geopolymer synthesis, testing, and characterization

Geopolymer syntheses were made by adding the alkaline activators to the zeolitic tuff samples and mixing for 3 min. The tuff/activator and sodium silicate/sodium hydroxide ratios were 1.75 and 3, respectively. After mixing, the fresh geopolymer paste was cast in a 50 × 50 × 50 mm cube mold (see Fig. 2). The specimens were removed from the molds, covered with film to prevent loss of moisture, and subjected to 7-, 28-, and 56-day curing times at 50 °C, following the procedure of Villa et al. [22] and Ozen and Alam [21] which gives better compressive strength.

In the mix design of the geopolymers, the NaOH molarity, curing temperature, tuff/activator and sodium silicate/sodium hydroxide ratios was optimized by the authors in [21,26] in order to achieve higher compressive strength. These values are in accordance to [22]. The geopolymers' compressive strength was determined at 7, 28, and 56 days using a universal testing apparatus (Utest 6410, load cell = 10 kN) at a loading rate of 6 Ns^{-1}. The strength values were obtained from the average of six measurements for each sample. Crushed pieces of the hardened zeolite-based geopolymer samples, taken after 28 days of curing, were also used for XRD and SEM-EDX analysis.

3. Results and discussion

3.1. Characterization of raw materials

Petrographical examination demonstrates that the very fine-grained CLI sample contains minor amounts of quartz, biotite, and smectite. The MOR and ANA samples exhibit glassy textures with partial alteration of mordenite and analcime, respectively; both contain authigenic feldspar (lamellar-twinned albite), volcanic glass, and clay mineral (smectite). The petrographical analysis indicates that the smectite content of the MOR and ANA samples is approximately 5% and 15 %, respectively, and the amount of volcanic glass is 30 % and less than 5%, respectively.

The quantitative phase compositions of the examined tuffs are displayed in Table 2. The CLI sample is very pure, with a zeolite content of 92 %. The MOR and ANA samples have zeolite contents of 30 % and 22 %, respectively. In the ANA sample, a considerable amount of feldspar (40 %) was detected. In the MOR and ANA samples, 38 % and 19 % of non-identified phases remain, respectively,

Table 2
Mineralogical composition of the examined tuffs.

Mineral	CLI	MOR	ANA
Clinoptilolite	**92**		
Mordenite		**30**	
Analcime			**22**
Quartz	2	15	18
Feldspar	2	17	40
Biotite	1		1
Amorphous*	3	38	19
Total	100	100	100
* Including smectite			

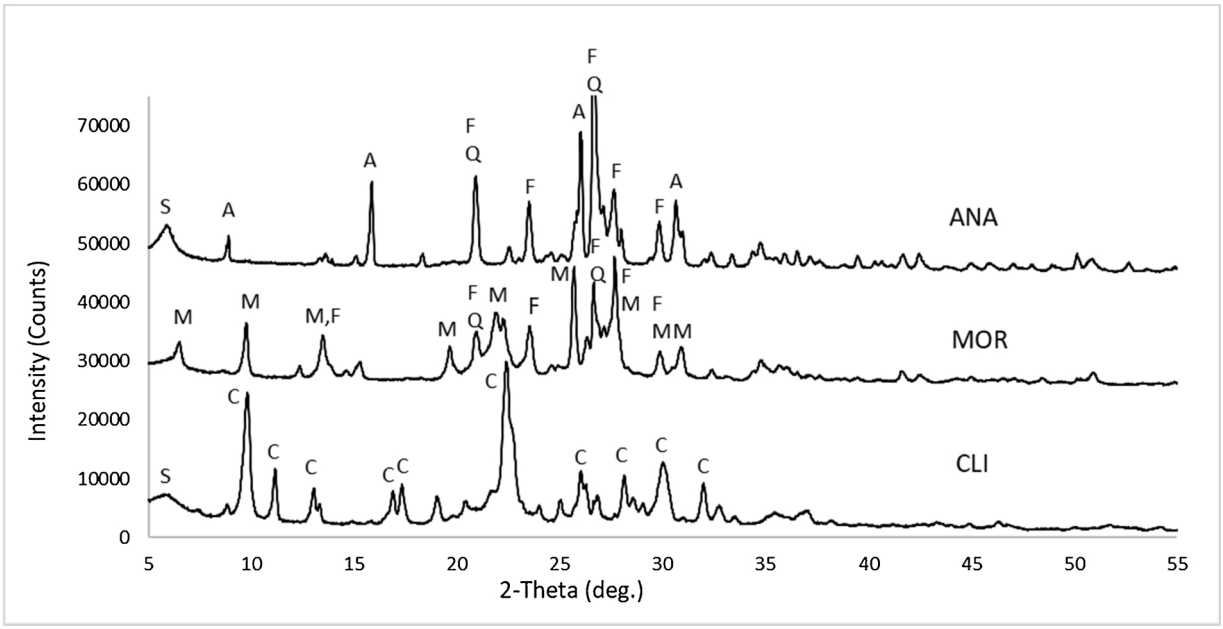

Fig. 3. XRD patterns of the CLI, MOR, and ANA samples (C: clinoptilolite, M: mordenite, A: analcime, Q: quartz, S: smectite, F: feldspar).

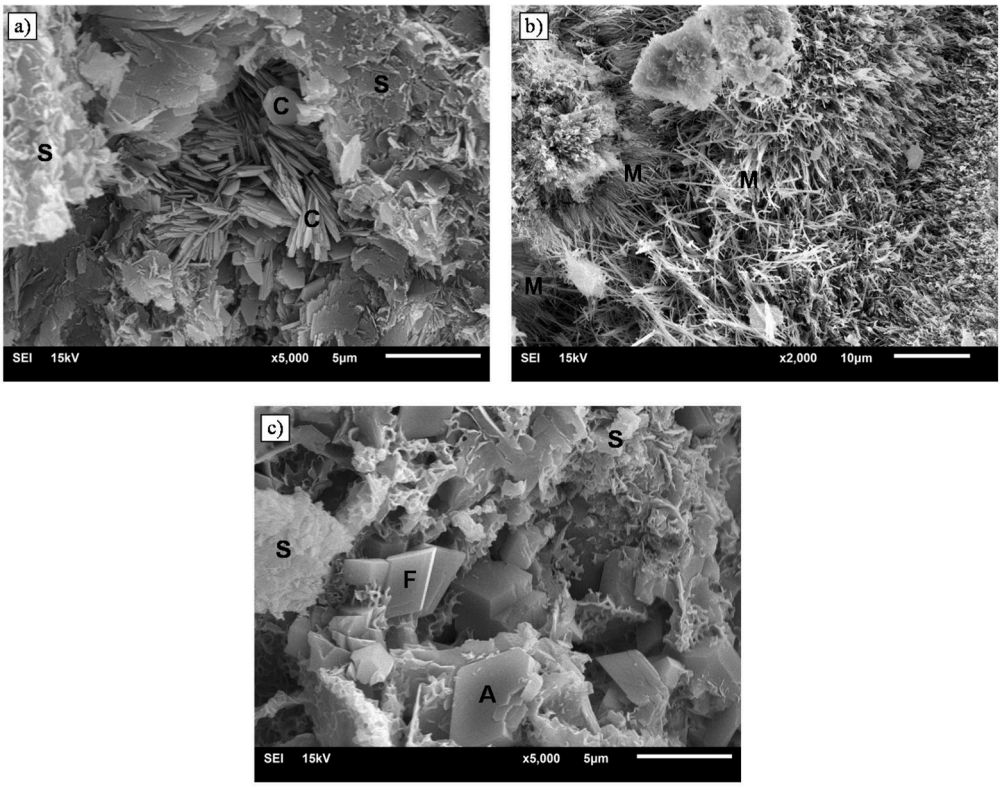

Fig. 4. SEM micrographs of the three starting materials: (a) the CLI sample displays tabular clinoptilolite (C) and honeycomb smectite (S); (b) the MOR sample displays needle-like crystals of mordenite (M); (c) the ANA sample displays cubo-octahedral analcime (A), honeycomb smectite (S), well-developed feldspar (F).

which the petrographic analysis suggests comprise volcanic glass and smectite.

Fig. 3 shows the XRD patterns of the three zeolite-bearing tuffs investigated. According to the XRD pattern, the major phase in the CLI sample is clinoptilolite (2θ of 11.16, 17.26, and 22.39, with *d*-spacing values of 7.92, 5.13, and 3.96 Å, respectively). Besides, smectite is present in CLI sample (2θ of 5.91 with a *d*-spacing value of 14.94 Å). In the MOR sample, the characteristic peaks of mordenite (2θ of 9.76, 19.67, and 25.66, with *d*-spacing values of 9.05, 4.51, and 3.46 Å), feldspar (2θ of 23.49 and 27.64, with *d*-spacing values of 3.78 and 3.22 Å), and quartz (2θ of 26.58 with a *d*-spacing value of 3.34 Å) are identified. In the ANA sample, analcime is recognized by its typical 3.42, 2.91, 2.49, and 4.84 Å peaks. Feldspar, quartz, and smectite are also evident in ANA sample (Fig. 3).

Fig. 4 displays the micromorphological features of the three starting materials. Aggregates of clinoptilolite are predominantly tabular in shape, with some displaying widths of 3–4 μm (Fig. 4a). Crystals of mordenite are needle-shaped, with some 2–10 μm long (Fig. 4b). Analcime is characterized by cubo-octahedral crystal, approximately 4–5 μm in diameter (Fig. 4c). Clinoptilolite, mordenite, and analcime crystals are generally associated with honeycomb smectite. Monoclinic feldspar also appears in the MOR and ANA samples.

3.2. Mechanical properties of natural zeolite-based geopolymers

The compressive strengths of the natural zeolite-based geopolymers (CLI, MOR, and ANA) cured at 50 °C for 7, 28, and 56 days are given in Fig. 5. The CLI sample possesses a higher compressive strength than both the MOR and ANA samples at all testing ages, which may be due to its smaller particle size and high BET-specific surface area. Additionally, the high content of reactive phase, namely clinoptilolite (92 %), may have caused the reaction to proceed at a faster rate, especially at later ages.

The mechanical development of the ANA sample is higher than that of the MOR sample, except after 7 days of curing (Fig. 5). The higher strength of the MOR sample than the ANA sample at the initial time (7 days) is attributed to its fineness, which indicates that particle size is more influential on the compressive strength of geopolymer mortars at early ages than later ages. The positive effect of finer particle sizes and, consequently, a higher BET-specific surface area on the early compressive strength of geopolymer mortars can be explained by the rapid and effective geopolymerization of smaller particles in the early reaction period. The difference in compressive strength between the MOR and ANA samples, despite their similar zeolite content, may be due to differences in phases other than the zeolites shown in the XRPD analysis. As seen in Table 2, the ANA sample contains a significant amount of feldspar (40 %), which is known to be active with regard to geopolymerization reaction [32,33]. Dissolving the feldspar structure results in the release of more chemical compounds from the starting material (ANA) and, therefore, an increase in the degree of geopolymeric reaction. Moreover, of the two parent materials, ANA has a higher proportion of smectite than MOR, as shown by the optical microscope. The depletion of the smectite's peak intensity indicates that it completely dissolves and plays a role in the geopolymerization reaction (discussed in section 3.3.1). In addition to these phases, volcanic glass, of which more is found in MOR (approximately 30 %) than ANA (approximately 5%), does not appear to react to a significant extent. Djobo et al. [34] have previously identified a very low dissolution of the glassy phase in volcanic ash in alkaline solution during geopolymerization. Namely, the total active phases participating in the geopolymerization reaction are 47 % for MOR (30 % mordenite and 17 % feldspar) and 77 % for ANA (22 % analcime, 40 % feldspar and 15 % smectite), creating the difference in the samples' compressive strength values. Hence, the reactivity of phases other than zeolites and the quantities of these phases in source materials also have a significant effect on strength development. Additionally, it is worth noting that the quantitative mineralogical characterization of starting material is very important step,

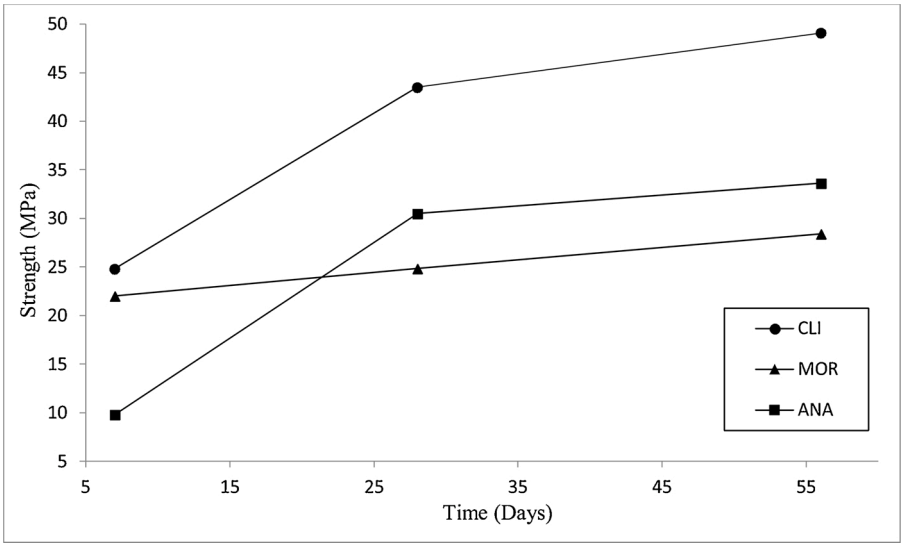

Fig. 5. The compressive strength of the geopolymers at 7, 28, and 56 days.

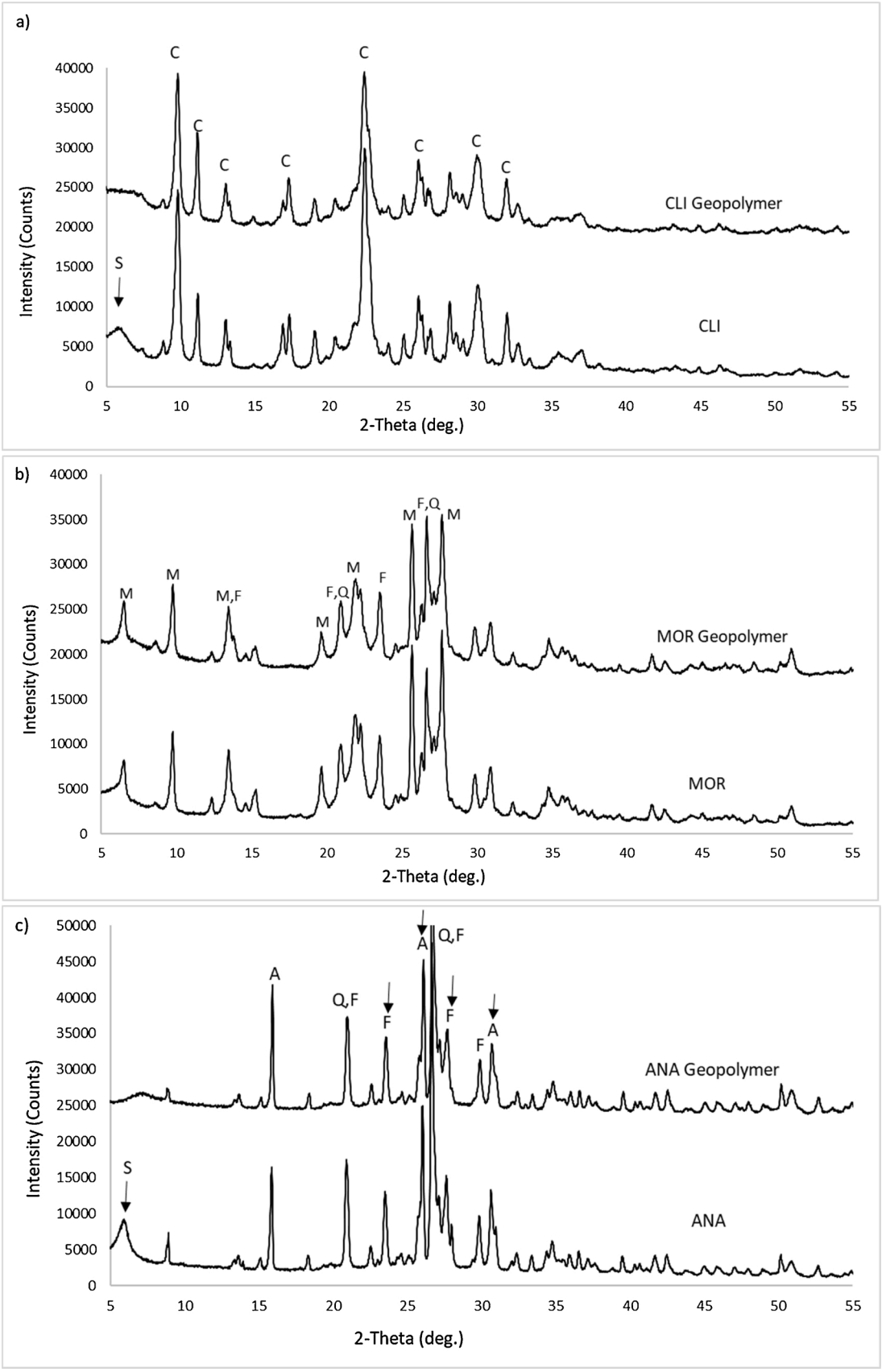

(caption on next page)

Fig. 6. The XRD patterns of (a) original clinoptilolite (CLI) and respective clinoptilolite-based geopolymer (CLI), (b) original mordenite (MOR) and respective mordenite-based geopolymer (MOR), (c) original analcime (ANA) and respective analcime-based geopolymer (ANA) after 28 days of curing.

which will help the researcher to interpret the results accurately. Furthermore, detail mineralogical characterization, which means not only phases present but also their quantity will guarantee the geopolymeric behavior of the materials.

The results also showed that although the strength of the ANA sample was very low at 7 days, it increased rapidly in the period from 7 to 28 days, in a similar way to the CLI sample, which thought to be due to the high quantitiy of phases attending to the geopolymeric reaction (77 % for ANA and 92 % for CLI). When 28 days of curing was reached, the rate of strength development slowed for both the CLI and ANA samples. The mechanical development of the MOR sample, on the other hand, steadily increased up to 56 days, which thought to be due to the low quantity of minerals participating in the reaction (47 %). The compressive strength of all the samples increased as the curing days increased, and the highest compressive strength of 49.1 MPA was recorded at 56 days of hydration for the CLI sample (Fig. 5).

3.3. Microstructural characteristics

3.3.1. XRD

XRD analysis was carried out to compare the phases present in the clinoptilolite-, mordenite-, and analcime-based geopolymers after 28 days of curing. The XRD patterns of the original materials, as well as their respective geopolymers, are shown in Fig. 6. As seen in Fig. 6, the crystalline zeolite phases originally existing in the aluminosilicate sources are also present in the synthesized geopolymers, though with reduced intensity (A slight reduction of the peak intensities of analcime from 13,560 cps to 11,778 cps at 2θ of 26.01 and from 4573 cps to 4440 cps at 2θ of 30.64 were detected). This suggests that all zeolites partially contribute to the geopolymerization reaction. However, in the XRD patterns of CLI geopolymer, the intensity of the partially reacted zeolite peaks present in all the geopolymers is further reduced compared to the XRD patterns of both the MOR and ANA geopolymers, indicating a higher dissolution of the alumino silicate structure of the clinoptilolite by the alkaline solution and a higher involvement of the geopolymeric reaction. It is worth noting that the amount of zeolite phase involved in the reaction is the highest for the CLI precursor (92 % clinoptilolite) as seen in Table 2. Hence, the reactivity of zeolites is not comparable. Yet, we can conclude that the reactivity of CLI precursor is higher than MOR and ANA precursor, which also supported by compressive strength analysis.

Furthermore, a broad, diffused halo of between 20–35° (2θ) exists in the patterns of the clinoptilolite- (CLI), mordenite- (MOR), and analcime (ANA)-based geopolymers, indicating amorphous gels in the geopolymers. The presence of amorphous phase formed as a result of the alkali activation of the zeolites have also been detected by other researchers. Villa et al. [22] reported the halo between 20–30° (2θ) indicating the presence of amorphous material after XRD analysis of clinoptilolite-based geopolymer. Baykara et al. [24], on the other hand, detected amorphous phase content by quantitative X-ray diffraction (QXRD) analysis examining mordenite-based geopolymer. Fig. 5 shows that the broad hump is more apparent for the CLI, which points to a higher degree of geopolymerization of CLI. This observation can explain why the CLI possesses higher mechanical development. A slight reduction of the peak intensities of feldspar (for example from 5701 cps to 5190 cps at 2θ of 23.49 and from 6687 cps to 5753 cps at 2θ of 27.64 between the original ANA raw material and respective ANA geopolymer) was also observed for original raw materials and respective MOR and ANA geopolymers (Fig. 6). Additionally, the smectite peak, detected in the XRD diagrams of CLI and ANA, does not appear after geopolymerization. The reduction of the peak intensity of feldspar and disappearance of the peak intensitiy of smectite evince that these phases also contribute to the geopolymerization reaction. The peak of quartz, however, remains almost constant, indicating that its activation is minimal. Nevertheless, the presence of quartz may enhance the particle packing and nucleation through the filler effect [35].

3.3.2. SEM/EDX

Fig. 7 shows the representative microstructural regions by SEM and the results of the chemical characterization by EDX of the three original raw materials. As Fig. 7 indicates, Si and Al are the main elements in clinoptilolite-rich tuff, which also contains Ca and K in lower concentrations. The elements of mordenite-bearing tuff are similarly dominated by Si and Al, with some Ca and approximately 2 wt.% of Na and K. The elements of analcime-bearing tuff are dominated by Si, Al, and Na and less than 2 wt.% of K. CLI sample is decidedly more siliceous than MOR and ANA samples. ANA sample is, as expected, definitely sodic and poor in calcium. The semi-quantitative Si/Al atomic ratio of the samples was 5 for CLI, 6.31 for MOR, and 5.51 for ANA.

Fig. 8 displays the micromorphological differences of the CLI, MOR, and ANA geopolymers after 28 days of activation. The SEM image of CLI reveals a completely smooth gel-like structure that is the densest and most homogenous of the three materials, followed by ANA and MOR, respectively. This is likely because of the further dissolution of the clinoptilolite found in CLI and increased formation of reaction product during geopolymerization. In addition, comparing the microstructural features of the CLI, MOR, and ANA geopolymers through a compressive strength analysis results in the following sequence: CLI > ANA > MOR; the presence of a well-developed gel-like structure acquired from the activation of zeolite-based geopolymers is expected to lead to higher compressive strength. While many microcracks can be seen in the micrograph of the CLI and ANA samples, much larger and more distinct cracks with many voids are evident in the MOR sample, which possesses lower mechanical development than the CLI and ANA geopolymers.

The results of the EDX analyses of the zeolite-based geopolymers are also displayed in Fig. 8. Resulting from the uniform texture and complex chemical composition of the zeolite-based geopolymer system, identification of the type of geopolymers cannot be made with EDX analysis. Instead, the semiquantitative chemical composition of the main matrix area presenting the gel-like texture was

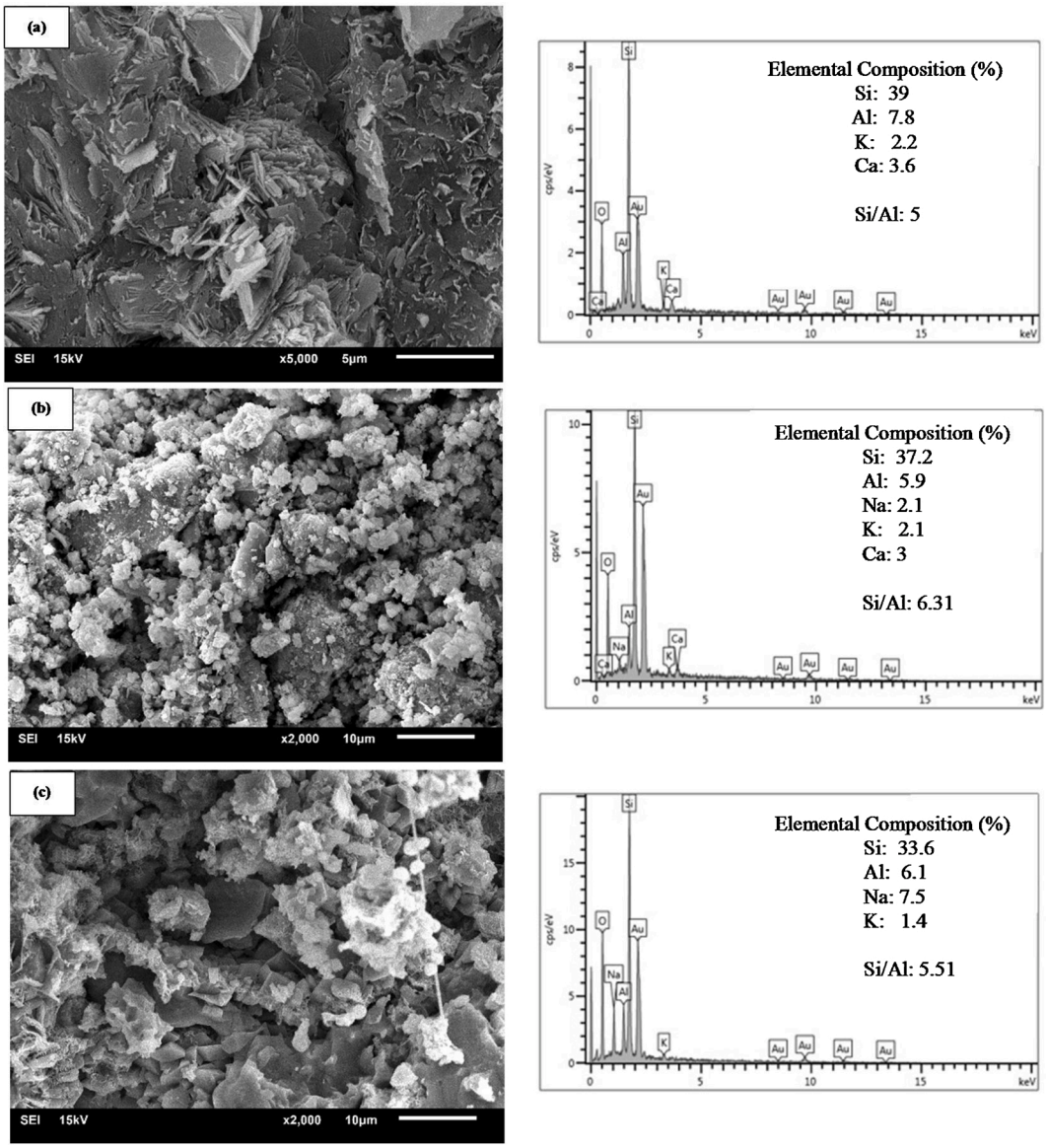

Fig. 7. SEM/EDX analyses of zeolite-bearing tuffs: (a) SEM micrograph of clinoptilolite-rich tuff (CLI) and chemical characterization by EDX of the CLI sample in general; (b) a SEM micrograph of mordenite-bearing tuff (MOR), and chemical characterization by EDX of the MOR sample in general; (c) a SEM micrograph of analcime-bearing tuff (ANA), and chemical characterization by EDX of the ANA sample in general.

determined. According to the analysis results, the major elements of the gel-like matrix are Si, Al, and Na. Therefore, the area of glassy matrix may be a geopolymeric gel comprising the main reaction product, which has similar chemical composition to gels in the existing literature [17,35]. Besides, an increment of Si/Al ratio and sodium incorporation in respect of starting raw materials were determined in the geopolymer product (see Table 3).

The results of the semiquantitative elemental analysis on selected spots in the geopolymeric gels present in the matrix are plotted as (Na + K+Ca + Fe + Mg)/Al against Si/Al, as shown in Fig. 9, which is helpful to understand the role of active phases involved in the geopolymeric reaction. Although the values of the Si/Al ratio of materials vary considerably (4.88–7.73), the most frequent Si/Al ratio of all the geopolymers is found in the range of 5.7–6.2, which is similar to the values of the Si/Al ratio stated by Villa et al. [22]. In general, the ANA sample has a higher Si/Al ratio than the CLI and MOR samples, whereas the MOR sample has a lower ratio. The differences in Si/Al ratio, which is most probably because of the different type of geopolymeric gel developed by activation of different type of precursors (clinoptilolite, mordenite, analcime in this case) were also stated by Nath [36] for different precursor materials. As clearly visible in Fig. 9, the Si/Al ratio of the CLI sample presents a narrow range of variation, while considerably variant Si/Al molar ratios were defined for the MOR and ANA samples. This narrow composition of CLI reflects the advanced nature of its gel structure in agreement with published literature [37]. In addition, the (Na + K+Ca + Fe + Mg)/Al ratio of CLI is higher than that of the MOR and

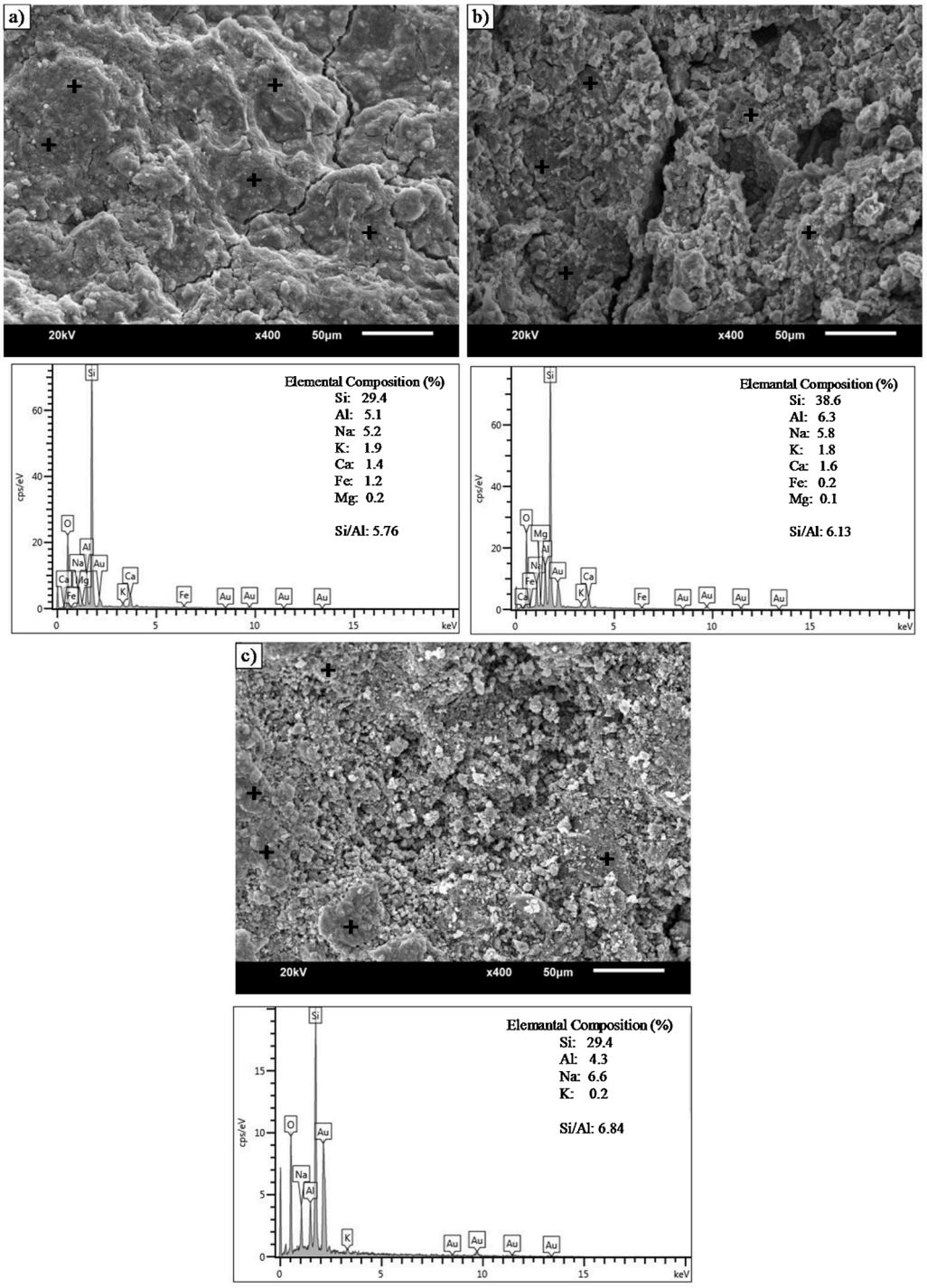

Fig. 8. SEM/EDX analyses of (a) CLI-G, (b) MOR-G, and (c) ANA-G samples.

ANA samples. During the geopolymerization process, the role of alkali metals in the reaction is essential [32]. As reported in the literature [38,39], some alkali metals are likely present in the geopolymer binder due to the dissolution of raw materials and the substitution of those species by geopolymeric reaction. For this reason, the higher (Na + K+Ca + Fe + Mg)/Al ratio of CLI is an indication of a higher dissolution and subsequently higher incorporation of those alkali metals into the geopolymeric gel structure, which leads to a higher modification of the geopolymeric gel structure, as a result of the presence of a highly reactive phase in the starting material. Furthermore, as seen in Table 3, CLI possesses higher Ca content than MOR and ANA samples. This simply means that CLI sample has more Ca containing geopolymer product, which increases the binding property and thus compressive strength of

Table 3
The results of the atomic compositions (semiquantitative) of geopolymeric gel presented in the matrix.

Sample		Si	Al	Na	K	Ca	Fe	Mg	Si/Al	(Na + K-Ca + Fe + Mg)/Al
	1	34.3	5.8	5.1	2.3	2.8	0.8	0.5	5.91	1.98
	2	33.4	5.6	5.5	1	2.6	0.6	0.5	5.96	1.82
CLI	3	31.7	5.4	6.5	1.9	1.3	0.1	0.4	5.87	1.89
	4	29.4	5.1	5.2	1.9	1.4	1.2	0.2	5.76	1.94
	5	35.9	5.9	6.6	2	1.9	0.6	0.1	6.08	1.90
	1	33.1	6.3	6.4	3.1	0.3	0.1	0	5.25	1.57
	2	33.6	6.1	6.5	1.4	0.8	0.1	0	5.51	1.44
MOR	3	38.6	6.3	5.8	1.8	1.6	0.2	0.1	6.13	1.51
	4	32.3	5.5	5.6	2.3	1.4	0.1	0	5.87	1.71
	5	27.3	5.6	6.3	2.9	0.9	0.1	0.1	4.88	1.84
	1	37.9	4.9	7.8	0.6	0.6	0.2	0	7.73	1.88
	2	29.4	4.3	6.6	0.2	0	0	0	6.84	1.58
ANA	3	34.9	5.4	8.4	0.4	0.3	0.1	0	6.46	1.70
	4	29.4	5.1	7.7	0.6	0.5	0.2	0.1	5.76	1.78
	5	33.5	5.6	7.6	0.6	0.4	0.2	0.1	5.98	1.59

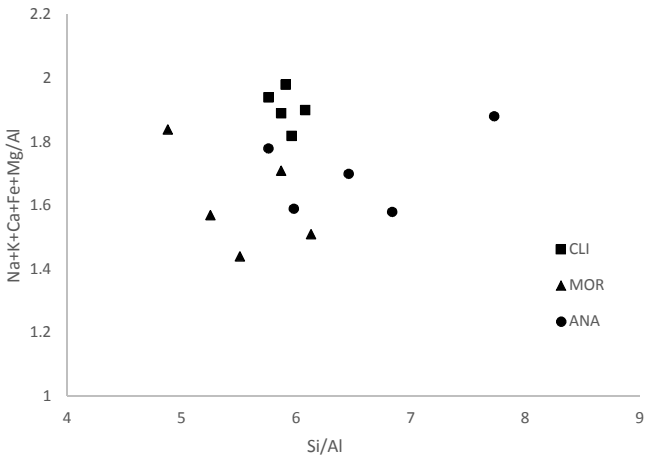

Fig. 9. Results of the EDX analysis plotted on the axes (Na + K+Ca)/Al vs. Si/Al ratios. The points correspond to the selected spots in Fig. 7.

resulting geopolymer as stated by [37].

The (Na + K+Ca + Fe + Mg)/Al ratio of the MOR and ANA geopolymers, on the other hand, are quite similar (Fig. 9). However, as seen in Table 3, the average Na composition of the geopolymeric gel in ANA is higher than in MOR, which is likely due to the Na ion contained in the original raw material. The Na may come not only from Na-rich analcime but also from feldspar (albite), which also contains Na ion in its structure. Feldspar group minerals are pozzolanic aluminosilicate materials, which can also be used in geopolymer synthesis [32]. According to Gonzalez-Garcia [40], after 28 days of curing at 40 °C, a natural pozzolan containing albite, anorthite, calcite, and quartz has the compressive strength of 13.2 MPa. It seems that in addition to analcime, feldspar also provides an alkali metal (Na) for the geopolymerization process at a certain stage of the reaction, reinforcing the gel structure and thus developing better compressive strength. Hence, it was concluded that active phases other than zeolites in the reaction mechanism are also crucial for the mechanical development of geopolymer material. Future work should examine at which stage of the reaction and how feldspar affects the geopolymeric reaction of raw materials containing zeolite.

Lastly, in literature, there are relevant works, which concluded optimal ratios for strength development of clinoptilolite- and mordenite-based geopolymers [21–26]. Gungor [26] also investigate the optimal ratios for anlacime-based geopolymer by investigating the tuff/activator and sodium silicate/sodium hydroxide ratios. Since this study aimed the research on focusing on comparing characterization of clinoptilolite-, mordenite-, and analcime-based geopolymers, suitable optimal ratios of the three geopolymers are selected from literature. However, there is scarcity of analcime-based geopolymers, in considering future work, it is also worth determining the detail effect of mix design of analcime-based geopolymers on strength development.

4. Conclusions

The analysis results demonstrate the potential use of clinoptilolite-, mordenite-, and analcime-bearing tuffs as aluminosilicate sources for the production of geopolymer cement. Clinoptilolite-based geopolymer has been found to be a more reactive, generating a high rate of reaction with respect to mordenite- and analcime-based geopolymer especially due to its smaller particle size, high BET-

specific surface area and high content of clinoptilolite (92 %).

It was shown that, in addition to the zeolite phase, other reactive components and their quantities also have a significant effect on geopolymerization. The higher mechanical development of the ANA than that of the MOR is attributed to presence of a significant amount of feldspar (in addition to clinoptilolite), which is known to be active with regard to geopolymerization reaction. The presence of quartz, on the other hand, may enhance the particle packing and nucleation through the filler effect. Thus, the authors suggest quantitative mineralogical characterization of raw materials, which will help the researcher to interpret the results accurately.

The difference in the mechanical and microstructural properties of natural zeolite-based geopolymers is attributed to the varying nature and mineralogical content of the starting materials. Furthermore, the different elemental compositions of the geopolymeric gels present in the matrix provide important information about the behavior of the active phases present in the original raw materials. The narrow composition of Si/Al ratio indicates the advanced nature of its gel structure. In addition, the higher Ca content of geopolymer products for CLI sample than MOR and ANA samples results higher compressive strength of CLI geopolymer than others. Lastly, it seems that in addition to analcime, feldspar also provides an alkali metal (Na) for the geopolymerization process at a certain stage of the reaction, reinforcing the gel structure and thus developing better compressive strength.

Declaration of Competing Interest

The authors declare that they have no known competing financial interests or personal relationships that could have appeared to influence the work reported in this paper.

Acknowledgements

This research was founded by TUBITAK as project number 215M787. Recep Tayyip Erdoğan University Central Laboratories are also gratefully acknowledged.

References

[1] G. Habert, C. Ouellet-Plamondon, Recent update on the environmental impact of geopolymers, RILEM Tech Let. 1 (2016) 17–23.
[2] J. Olivier, K. Schure, J. Peters, J, Trends in Global CO_2 and Total Greenhouse Gas Emissions, PBL Netherlands Environmental Assessment Agency, 2017.
[3] J. Davidovits, Properties of Geopolymer Cements, Proceedings First International Conference on Alkaline Cements and Concretes, vol. 1, SRIBM, Kiev, Ukraine, 1994, pp. 131–149.
[4] B.C. McLellan, R.P. Williams, J. Lay, A. van Riessen, G.D. Corder, Costs and carbon emissions for geopolymer pastes in comparison to ordinary portland cement, J. Cleaner Prod. 19 (2011) 1080–1090.
[5] P. Duxson, A. Fernandez-Jimenez, J.L. Provis, G.C. Lukey, A. Palomo, J.S.J. Van Deventer, Geopolymer technology: the current state of the art, J. Mater. Sci. 42 (2007) 2917–2933.
[6] Z.F. Wang, S.L. Shen, G. Modoni, A. Zhou, Excess pore water pressure caused by the installation of jet grouting columns in clay, Comp. Geotech. 125 (2020) 103667.
[7] Z.F. Wang, S.L. Shen, G. Modoni, Enhancing discharge of spoil to mitigate disturbance induced by horizontal jet grouting in clayey soil: theoretical model and application, Comp. Geotech. 111 (2019) 222–228.
[8] X.X. Liu, S.L. Shen, Y.S. Xu, A. Zhou, A diffusion model for backfill grout behind shield tunnel lining, Int. J. Numer. Anal. Meth. Geomech. 45 (4) (2020) 457–477.
[9] S.L. Shen, P.G.A. Njock, A. Zhou, H.M. Lyu, Dynamic prediction of jet grouted column diameter in soft soil using Bi-LSTM deep learning, Act. Geotech. 16 (2020) 303–3015.
[10] Y. Wu, B. Lu, T. Bai, H. Wang, F. Du, Y. Zhang, L. Cai, C. Jiang, W. Wang, Geopolymer, green alkali activated cementitious material: synthesis, application and challenges, Constr. Build. Mater. 224 (2019) 930–949.
[11] R. Gopalakrishnan, K. Chinnarahu, Durability of ambient cured alumina silicate concrete based on slag/fly ash blends against sulfate environment, Constr. Build. Mater. 204 (2019) 70–83.
[12] Y. Zhao, T. Shi, L. Cao, L. Kan, M. Wu, Influence of steel slag on the properties ofalkali-activated fly ash and blast-furnace slag based fiber reinforced composites, Cem. Conc. Com. 116 (2021), 103875.
[13] N. Ismail, H. El-Hassan, Development and characterization of fly ash-slag blended geopolymer mortar and lightweight concrete, J. Mater. Civil Eng. 30 (2018) 126–135.
[14] Y. Ding, C.J. Shi, N. Li, Fracture properties of slag/fly ash-based geopolymer concrete cured in ambient temperature, Constr. Build. Mater. 190 (2018) 787–795.
[15] U.S. Agrawal, S.P. Wanjari, D.N. Naresh, Characteristic study of geopolymer fly ash sand as a replacement to natural river sand, Constr. Build. Mater. 150 (2017) 681–688.
[16] S.Y. Oderji, B. Chen, M.R. Ahmad, S.F.A. Shah, Fresh and hardened properties of one-part fly ash-based geopolymer binders cured at room temperature: effect of slag and alkali activators, J. Cleaner Prod. 225 (2019) 1–10.
[17] J. He, J. Zhang, Y. Yu, G. Zhang, The strength and microstructure of two geopolymers derived from metakaolin and red mud-fly ash admixture: a comparative study, Constr. Build. Mater. 30 (2012) 80–91.
[18] Q. Wan, F. Rao, S. Song, D.F. Cholico-Gonzalez, N.L. Ortiz, Combination formation in the reinforcement ofmetakaolin geopolymers with quartz sand, Cem. Concr. Compos. 80 (2017) 115–122.
[19] H.T. Kouamo, A. Elimbi, J.A. Mbey, C.J.N. Sabouang, D. Njopwouo, The effect of adding alumina-oxide to metakaolin and volcanic ash on geopolymer products: a comparative study, Constr. Build. Mater. 35 (2012) 960–969.
[20] H.K. Tchakoute, A. Elimbi, E. Yanne, C.N. Djangang, Utilization of volcanic ashes for the production of geopolymers cured at ambient temperature, Cem. Concr. Compos. 38 (2013) 75–81.
[21] S. Ozen, B. Alam, Compressive strength and microstructural characteristics of natural zeolite-based geopolymer, Period. Polytech. Civ. Eng. 62 (1) (2018) 64–71.
[22] C. Villa, E.T. Pecina, R. Torres, L. Gomez, Geopolymer synthesis using alkaline activation of natural zeolite, Constr. Build. Mater. 24 (2010) 2084–2090.
[23] İ. Tekin, Properties of NaOH activated geopolymer with marble, travertine and volcanic tuff wastes, Constr. Build. Mater. 127 (2016) 607–617.
[24] H. Baykara, M.H. Cornejo, R. Murillo, A. Gavilanes, C. Paredes, J. Elsen, Preparation, characterization and reaction kinetics of green cement: ecuadorian natural mordenite-based geopolymers, Mater. Struct. 50 (2017) 188.
[25] A. Nikolov, H. Nugteren, I. Rostovsky, Optimization of geopolymers based on natural zeolite clinoptilolite by calcination and use of aluminate activators, Constr. Build. Mater. 243 (2020), 118257.

[26] D. Gungor, Doğal Zeolit Bazlı Geopolimerlerin Özellikleri, MSc Thesis, Recep Tayyip Erdoğan University, Rize, Turkey, 2019.
[27] D. Bondar, C.J. Lynsdale, N.B. Milestone, N. Hassani, A.A. Ramezanianpour, Effect of type, form and dosage of activators on strength of alkali-activated natural pozzolans, Cem. Concr. Compos. 33 (2) (2011) 251–260.
[28] R.I. Yousef, B. El-Eswed, M. Alshaaer, F. Khalili, H. Khoury, The influence of using Jordanian natural zeolite on the adsorption, physical, and mechanical properties of geopolymers products, J. Hazard. Mater. 165 (2009) 379–387.
[29] S. Ozen, Pozzolanic Activity of Natural Zeolites: Mineralogical, Chemical and Physical Characterizastion and Examination of Hydration Products, PhD Thesis, Middle East Technical University, Ankara, Turkey, 2013.
[30] American Society for Testing and Materials (ASTM) # C204-11e1, Standard Test Methods for Fineness of Hydraulic Cement by Air-Permeability Apparatus, ASTM International, West Conshohocken, PA, (USA), 2011.
[31] D.L. Bish, J.E. Post, Quantitative mineralogical analysis using the Rietveld fullpattern fitting method, J. Bone Miner. Res. 78 (1993) 932–940.
[32] H. Xu, J.S.J. van Deventer, Factors affecting the geopolymerization of alkali-feldspars, Trans. Soc. Min. Metall. Explor. Inc 19 (4) (2002) 209–214.
[33] D.M. Gonzalez-Garcia, L. Tellez-Jurado, F.J. Jimenez-Alvarez, H. Balmori-Ramirez, Structural study of geopolymers obtained from alkali-activated natural pozzolan feldspars, Interceram - Int. Ceram. Rev. 43 (2017) 2606–2613.
[34] J.N.Y. Djobo, A. Elimbi, H.K. Tchakoute, S. Kumar, Reactivity of volcanic ash in alkaline medium, microstructural and strength characteristics of resulting geopolymers under different synthesis conditions, J. Mater. Sci. 51 (2016) 10301–10317.
[35] C.K. Yip, G.C. Lukey, J.S.J. van Deventer, The coexistence of geopolymeric gel and calcium silicate hydrate at the early stage of alkaline activation, Cem. Concr. Res. 35 (2005) 1688–1697.
[36] S.H. Nath, Geopolymerization behavior of ferrochrome slag and fly ash blends, Constr. Build. Mater. 181 (2018) 487–494.
[37] S. Songpiriyakij, T. Kubprasit, C. Jaturapitakkul, P. Chindaprasirt, Compressive strength and degree of reaction of biomass- and fly ash-based geopolymer, Constr. Build. Mater. 24 (3) (2010) 236–240.
[38] J. Moon, S. Bae, K. Celik, S. Yoon, K.H. Kim, K.S. Kim, P.J.M. Monteiro, Characterization of natural pozzolan-based geopolymeric binders, Cem. Concr. Compos. 53 (2014) 97–104.
[39] T. Bakharev, Geopolymeric materials prepared using Class F fly ash and elevated temperature curing, Cem. Concr. Res. 35 (2005) 1224–1232.
[40] D.M. Gonzalez-Garcia, L. Tellez-Jurado, F.J. Jimenez-Alvarez, H. Balmori-Ramirez, Structural study of geopolymers obtained from alkali-activated natural pozzolan feldspars, Ceram. Int. 43 (2017) 2606–2613.